Nanoscale

Cite this: *Nanoscale*, 2011, **3**, 2768

www.rsc.org/nanoscale

REVIEW

Recent progress on surface pattern fabrications based on monolayer colloidal crystal templates and related applications

Shikuan Yang and Yong Lei*

Received 19th March 2011, Accepted 7th April 2011
DOI: 10.1039/c1nr10296f

This review summarizes the recent progress toward the fabrication of surface patterns depending on the monolayer colloidal crystal templates. Based on the structural differences of the acquired surface patterns, various synthesis routes are introduced in detail. The diverse device applications of the synthesized surface patterns are also summarized, including sensors, energy-related devices, field emissions, wettability control, and so on. Future research should focus on surface patterns composed of multiple-layered structures and hybrid materials, and the widening of their application explorations.

1. Introduction

Surface patterning fabrication is a prerequisite step to synthesize practical devices. Different lithographic approaches have been adopted to prepare surface patterns, including optical lithography, electron and focused ion beam lithography, and so forth.[1–5] Microcontact printing[6–8] and molding methods[9,10] are also harnessed in the preparation of surface patterns. In recent years, self-assembly techniques have been emerged as practical routes to prepare large-scale ordered nanostructures. Especially, patterning colloidal micro- and nanoparticles into ordered arrays has attracted much attention. So far the fabrication strategies of highly monodispersed micro- and nanoparticles [*e.g.*, polystyrene (PS) spheres, poly(methyl methacrylate), silica] are very

Institute of Materials Physics and Center for Nanotechnology, University of Muenster, Muenster, 48149, Germany. E-mail: yong.lei@uni-muenster.de

Shikuan Yang

Shikuan Yang obtained his PhD degree from the Institute of Solid State Physics, Chinese Academy of Sciences in 2009. His PhD thesis mainly focused on the fabrication of quantum dots by laser ablation in liquid medium. In 2009, he joined Prof. Yong Lei's group in the University of Muenster as a postdoctoral scientist. He has authored and co-authored more than 20 refereed journal publications. Now, his main research concentrates on surface nano-patterning using monolayer polystyrene sphere templates, and the related device applications.

Yong Lei

Yong Lei received his PhD in the Chinese Academy of Science in 2001. After two-year post-doctoral research in the Singapore–MIT Alliance, he worked in Karlsruhe Research Center in Germany as an Alexander von Humboldt Fellow. In 2006, he joined the Department of Physics at the University of Muenster in Germany as a group leader. He was appointed as a Professor in 2009 in the same university. He is a successful awardee of the prestigious European Research Council Funding. He also received some research prizes for his contributions in surface nano-structuring field. His major research interests include surface nano-structuring and patterning, template-fabrication of 1D nanostructures, structure-related properties of regular surface and 1D nanostructures and their device applications. He has authored more than 70 scientific publications, and so far his publications have received more than 1400 citations according to the SCI database.

mature; for example, PS spheres with diameters from about 100 nm to 5 μm are commercially available with size deviations smaller than 5%. These make it easy to prepare large-scale uniformly structured monolayer colloidal crystal (MCC) templates at very low cost and in a very time-efficient manner. Therefore, the MCC template-based protocols of surface patterning synthesis have attracted significant research interest, due to its low-cost, high throughput, easy structural controllability, and high reproducibility.[11–15] The MCC templates can be formed with organic [*e.g.*, polystyrene (PS) spheres] or inorganic (*e.g.*, silica) spheres. Normally, the spheres are hexagonally arranged in the template to form a monolayer array, which can be realized by many routes, such as spin-coating, drop-casting, dip-coating, evaporating, and dielectrophoresis.[11–15] Using the MCC templates as masks or molds (for evaporation, etching, imprinting, and deposition) a large number of surface patterns (including two-dimensional arrays)[16,17] have been synthesized with different building blocks, *e.g.*, rods, particles, hollow spheres, crescents, rings, and disks.

Among different MCC patterning techniques, the "colloidal lithography" method is well-known and has been widely used to fabricate honeycomb arrays of triangular or spherical particles. It is a simple and inexpensive technique to prepare surface patterns with good reproducibility. During the etching processes (*e.g.*, reactive ion etching) of the substrate (*e.g.*, Si wafer) covered by the MCC template, nanopillar arrays can be generated due to the protection of the spheres in the MCC template. By depositing materials on free-standing MCC templates at the air/water interface, porous membranes or bowl arrays can be synthesized. Through control of nucleation on the spheres in the MCC template during the electrochemical deposition process, free-standing particle arrays are prepared, which is very difficult to obtain by wet-chemical approaches. Also, the as-prepared close-packed MCC templates can be changed into non-close-packed ones by plasma etching, supplying more flexibility to adjust the array parameters. The small spacing between neighboring PS spheres induced by the plasma etching on the MCC templates is very important in some application areas, such as in surface enhanced Raman scattering (SERS) detections and field emissions. Furthermore, the MCC-prepared surface patterns combine the merits of both the building units and the geometry of the array. And the manipulation of the geometrical location of the building units in the ordered array is of prime importance to optimize the device performances of surface patterns. The obtained surface patterns can be used in a wide variety of applications, such as in data storage, sensing, and energy-related areas, to name but a few.

There are a few review articles covering the fabrication of surface patterns with MCC templates.[13–15] However, a review regarding the manufacturing techniques of MCC surface patterning and the corresponding device applications is still lacking. Moreover, there have been many new progresses in the field of MCC surface patterning in the past few years. In this review, we will summarize the very recent and representative developments (within the past 5 years) of MCC (mainly focusing on the PS sphere templates) surface patterning techniques, focusing on their applications in various areas, such as sensing, energy-related fields, field emissions, optical and magnetic regions. We classify the fabrication protocols according to the geometric differences of the obtained surface patterns. Seven sections are included in this review articles. In section 2, general fabrication protocols of surface patterns based on MCC templates are schematically illustrated, which can facilitate the understanding of the subsequent contents. Section 3 demonstrates various protocols that can be used to synthesize honeycomb arrays are introduced. Section 4 summarizes the distinguished techniques to fabricate hexagonally arranged arrays composed of different building blocks. The techniques to prepare non-close-packed MCC templates and the related surface patterning fabrications are introduced in section 5. In section 6, the properties and device applications of the surface patterns are presented. Finally, section 7 gives a summary and future outlook of the MCC surface patterning technique.

2. Schematic illustrations of the MCC surface patterning approaches

Generally, according to the topologic structures of the surface patterns, honeycomb and hexagonally structured arrays can be prepared by MCC templates. Honeycomb arrays of triangular nanoparticles can be synthesized (see route 1 in Scheme 1) by using MCC templates as masks during thermal evaporations (details can be found in section 3.1). After thermal treatment of the triangular nanoparticles, they can be evolved into roundish nanoparticles (route 1′ in Scheme 1). These metallic nanoparticles can be used as catalysts for leading the growth of one-dimensional (1D) nanorods (route 1″ in Scheme 1) *via* physical vapor deposition (PVD) methods (details are shown in section 3.2). When the MCC template is rotated during the evaporation process, honeycomb array of nanorings will emerge (route 2 in Scheme 1; discussed in section 3.3). Besides these honeycomb arrays induced by the MCC templates, hexagonally arranged nanostructures can also be prepared. Through firstly replicating the MCC template with silica sol followed by removing the PS spheres, bowl arrays can be generated. Subsequently, a thin layer of metallic films is evaporated on the surface of the bowl template. After thermal heating treatment, hexagonally arranged nanodots appear (see route a in Scheme 1 and the content in section 4.1). We call this fabrication method "template-confined dewetting process", which is a powerful technique to synthesize hexagonally arranged nanodot arrays. This method supplies a complementary way to the conventional "colloidal lithography" approach in designing surface nano-patterns. Hexagonally arranged nanopillar arrays are also available based on pulsed laser deposition (PLD) on the MCC templates (route b in Scheme 1; section 4.2). Considering the spherical shape of the PS spheres, various deposition methods (*e.g.*, electrochemical deposition) are adopted to "paint" materials on the surface of the PS spheres (route c in Scheme 1). After removing the PS spheres, hollow sphere arrays are realized (route c′ in Scheme 1 and the content in section 4.3). Bowl arrays can also be synthesized by the MCC templates, either through milling the hollow spheres or *via* direct thermal evaporation on the top surface of the PS spheres (see route d in Scheme 1 and section 4.4). Wet-chemical strategies are used to fabricate hexagonally located nanoring arrays (see route e in Scheme 1 and section 4.5). Conducting thermal evaporation with tilted MCC templates, nanocrescents will be formed at one side of the interfaces between the PS spheres and

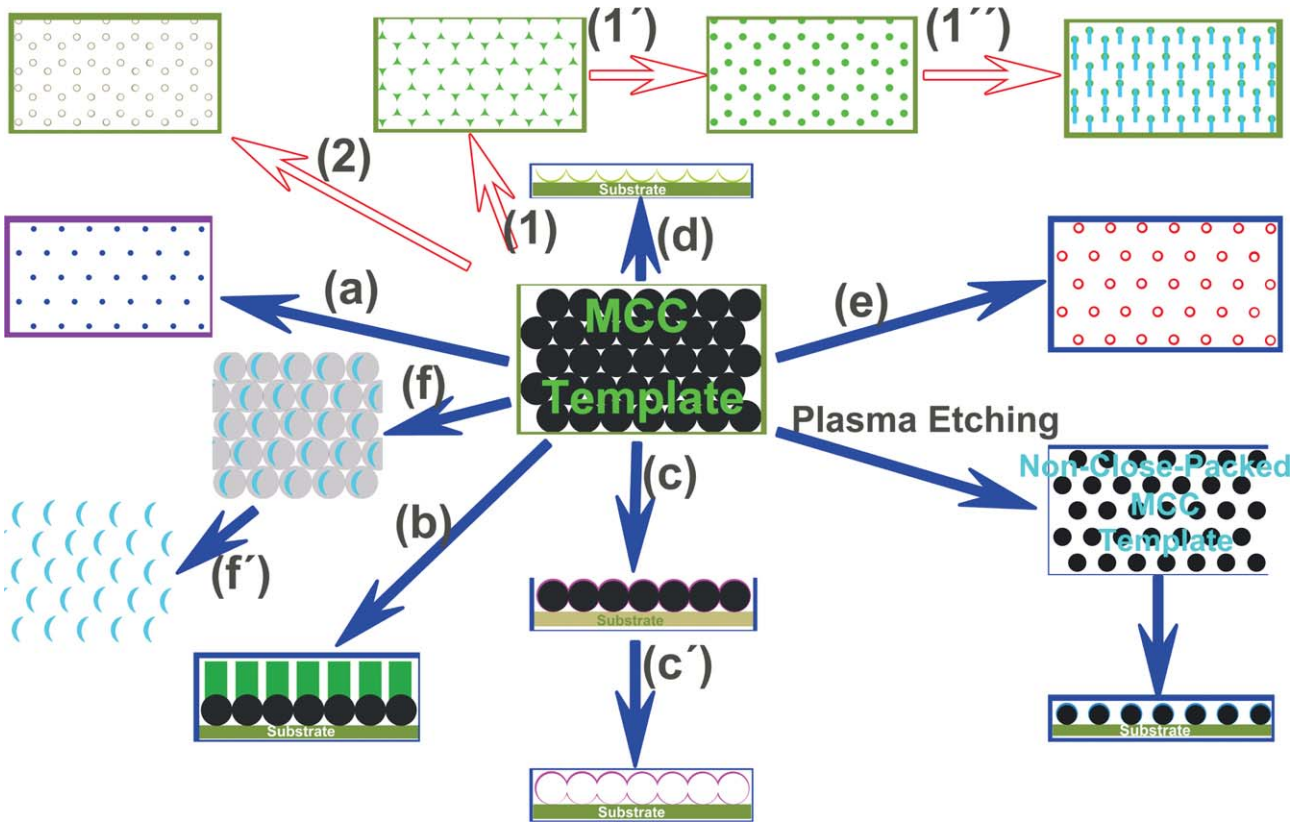

Scheme 1 Schematic demonstration for the MCC surface patterns with different geometrical structures. Routes 1 and 2 are related to honeycomb array fabrications. Routes a to e correspond to hexagonal array synthesis.

the beneath substrate (route f in Scheme 1). Nanocrescent arrays appear after dissolving the PS spheres (route f′ in Scheme 1 and section 4.6). Importantly, the MCC templates can be changed into non-close-packed ones by plasma etching treatment (see Scheme 1). The spacing between adjacent PS spheres is dependent on the time of the plasma etching treatment. The non-close-packed MCC templates are robust platforms to prepare nanostructure arrays with certain and controllable spacings between the building blocks in the array. In some applications, nanoscale crevices between neighboring units are of prime importance. For example, "hot spots" usually situate at nanoscale crevices, which are highly sensitive sites in SERS detections. In field emission applications, because of the screening effect between closely located nanostructures, certain distances between neighboring nanostructures are crucial for optimizing the field emission performances. Surface nano-patterns with the other complex geometries can also be acquired. But these techniques are often very complicated and with low reproducibility. These fabrication routes are not included in this review article.

3. Honeycomb arrays

3.1 Triangular nanoparticles

Nanosphere lithography (NSL), also known as "colloidal lithography" and "natural lithography", was first used for the fabrication of Pt honeycomb arrays.[18] After that, this method was successfully extended to fabricate large area surface nanopatterns.[19,20] A NSL process developed by van Duyne *et al.* had been widely used to prepare honeycomb arrays composed of triangular nanoparticles of different materials.[21] The LSPR properties of the obtained metallic patterns were studied and biosensors depending on the SERS from the metallic patterns were designed. Fig. 1a shows honeycomb array of triangular gold nanoparticles synthesized with 1 μm sized PS spheres. After heating at elevated temperatures (*e.g.*, 400 °C), the triangular nanoparticles can evolve into spherical nanoparticles (Fig. 1b). The constituent triangular nanoparticles have similar sizes and shapes in the surface patterns prepared with the NSL method. The morphology of the triangular nanoparticles and their particle-to-particle distance can be conveniently adjusted. Based

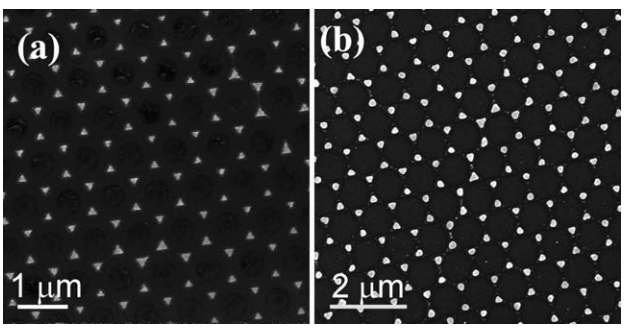

Fig. 1 SEM images of the honeycomb array composed of gold triangular (a) and spherical nanoparticles (b).

on tuning the size of the truncated tetrahedral silver nanoparticles, the surface plasmon resonance (SPR) could be manipulated in a broad range.[22] When the NSL-fabricated Ag nanotriangles suffered from an electrochemical treatment, the morphology would be changed by the oxidation process. The etching process took place first at the bottom edges, and then triangular tips, at last out-of-plane height. Simultaneously, the LSPR shifted from less than 600 to more than 900 nm.[24] Similarly, the LSPR properties of Cu triangle arrays were studied.[25] A gold honeycomb array was prepared by El-Sayed *et al.* with the same technique, showing strong infrared absorption.[26] Interestingly, heterogeneous binary arrays of nanoparticles could also be acquired by the NSL approach with different incidence angles during the metal evaporation processes.[27]

3.2 Nanorods

The honeycomb arrays shown in section 3.1 could be used as catalysts to trigger the growth of 1D nanostructures such as carbon nanotubes. Large area photonic crystals depending on periodic arrays of carbon nanotubes were obtained (Fig. 2a).[28] With similar concept, molecular beam epitaxy was performed to synthesize Si nanowires catalysized by gold honeycomb arrays.[29] Glancing angle deposition (GLAD) is a technique to carry out thermal evaporations, where the incident flux impinges on the substrate from an oblique angle (generally >80°). Based on the GLAD combining with the MCC template patterning, Gall *et al.* have done a series of works. Among them, using a honeycomb array obtained by NSL methodology as the starting substrate, a Ta nanopillar array was acquired with a honeycomb-like structure (Fig. 2b).[30] Electrochemical deposition was also adopted in the fabrication of honeycomb arrayed nanorods of ZnO (Fig. 2c).[31] This was ascribed to the preferential nucleation on the beneath substrate instead of on the surface of the PS spheres. Moreover, the array structure could be tailored by the deformation of PS spheres *via* heating treatment of the MCC templates. The density, uniformity, and shape of the nanorods were tailorable through varying the template size, the PS deformation degree, and the electrolyte composition. It was also found that the field emission property of the ZnO nanorods was highly dependent on their structural parameters. Nanorod arrays with a low turn-on electric field of 1.8 V μm^{-1}, a high field-enhancement factor of 5750 and an emitting current density up to 2.5 mA cm^{-2} were successfully obtained. These supplied good candidate materials for cold-cathode-based electronics. Moreover, honeycomb arrays of tapered ZnO nanorods were fabricated by a wet chemical growth method with MCC templates as a mold in zinc precursor solution, as shown in Fig. 2d.[32]

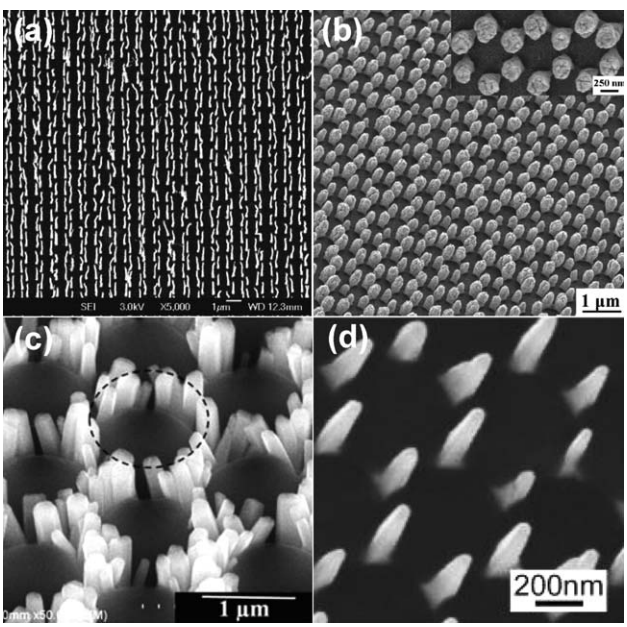

Fig. 2 Honeycomb array of nanopillars. (a) Carbon nanotube array synthesized by chemical vapour deposition with honeycomb array of metal nanoparticles as catalyst. (b) Ta nanopillar array synthesized by GLAD with honeycomb array of Cr nanoparticles prepared by NSL. (c) ZnO nanopillar array fabricated by electrochemical deposition approach using MMC template as a mask. (d) Tapered ZnO nanopillar array synthesized through wet chemical growth technique. ((a) ref. 23, (b) ref. 25, (c) ref. 26, (d) ref. 27.)

3.3 Nanorings

Besides nanoparticle arrays, the NSL method can also be harnessed to fabricate nanoring arrays. In brief, the tilted (tilt angle around 25°) MCC template was rotated during the thermal evaporation process, as schematically shown in Fig. 3a. This method allows the preparation of large-scale, highly ordered nanoring arrays of various materials, such as Fe, Co and Ni.[33,34] Recently, the response of noble metal nanostructures to optical light has attracted much scientific research, due to their application potentialities in LSPR sensing and photothermal therapies. The LSPR performance is dependent on both the structures and the arrangement of the noble metal nanostructures (due to the LSPR coupling and hybridization between closed located nanostructures). Au nanoring arrays were prepared with this method, as shown in Fig. 3b.[35] The prepared Au nanoring arrays showed interesting LSPR evolutions as the structure varied, which could be qualitatively understood by quasi-static formulas and taking into account of the oscillator strengths. The optical evolutions were in good agreement with the simulation results.[30] These large-scale gold nanoring arrays could be cheap

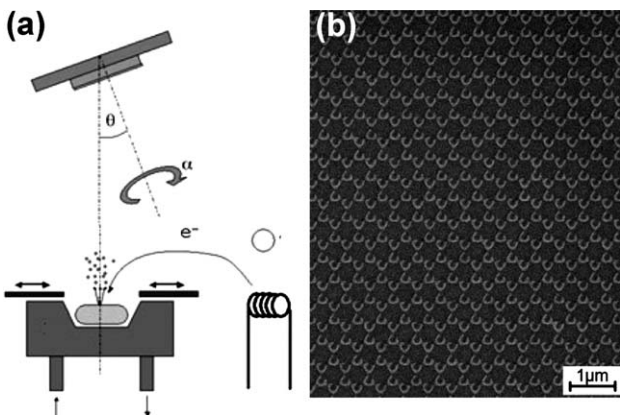

Fig. 3 (a) Schematic illustration for the fabrication of nanoring arrays. (b) Gold nanoring array. ((a) ref. 28, (b) ref. 30.)

metamaterials that can be used in lenses and optical cloaking devices.[35]

4. Hexagonal array

The spatial configuration plays a dominate role in defining some properties of the surface patterns. Therefore, exploration of the fabrication routes toward arrays with different geometries is of crucial importance. In this section, various techniques that can be used to prepare hexagonal arrays of nanodots, nanorods, nanorings, nanocreascents, and the others will be summarized.

4.1 Nanodots

Thin films evaporated on substrates are usually thermodynamically unstable.[36–38] Various methods have been explored to stabilize the evaporated thin film, such as the introduction of a transition layer (*e.g.*, evaporate a thin layer of Cr before the deposition of Au on the Si wafer). However, the instability of the thin film also brings a possibility to synthesize the ordered surface patterns. Depending on this concept, we developed a "template-confined dewetting process" to prepare hexagonally arranged nanodot arrays. The whole synthesis route is schematically shown in Scheme 2. At the beginning, silica sol was infiltrated to the interstitial spaces of the MCC template, and then bowls emerged after removing the PS spheres, as shown in Fig. 4a. A thin layer of metal film was further deposited on the surface of the bowl array. Consequent annealing treatments under elevated temperatures (*e.g.*, 300 °C, 350 °C and 400 °C) results in morphological evolution from continuous film to separated disks and further to hexagonally arranged nanodot arrays (Fig. 4b–4d). The side view of the morphological evolutions of the metallic films is shown in Scheme 3. Under thermal treatment at relative lower temperature, surface patterns composed of disk-like structures formed. The size, morphology and interparticle distance in the ordered array can be adjusted by changing the thickness of the evaporated film, heating temperatures, and selection of different sized MCC templates (*e.g.*, PS diameter). Importantly, the size of the nanodot can be precalculated (by the volume of the metal film evaporated in a single bowl). That is the diameter of nanoparticles ($2r$) can be calculated as a function of the bowl size ($2R$) and the thickness of the metallic film (H):

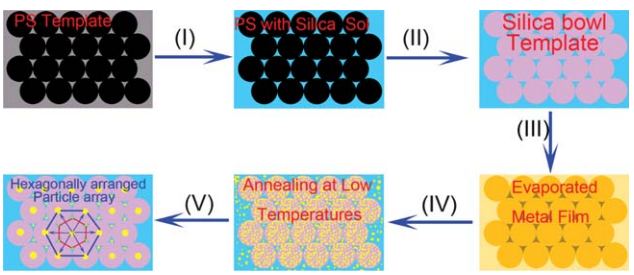

Scheme 2 Process flow of the fabrication of metallic surface nano-patterns through template-confined dewetting process. (I) Infiltration of silica sol. (II) Remove PS spheres and the formation of silica bowl templates. (III) Evaporating a layer of metal film. (IV) Annealing at low temperatures. (V) Heating at high temperatures resulting in the formation of hexagonally arranged nanoparticle arrays.

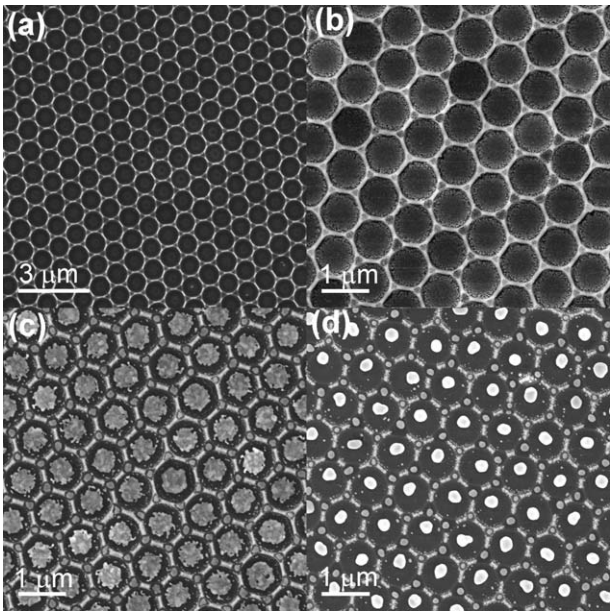

Fig. 4 Template-confined dewetting process to prepare different surface patterns. (a) Bowl template; (b) to (d) shape transformation of the gold film in bowls.

$$\pi R^2 H = 4/3\pi r^3 \quad (1)$$

This is a general method to prepare hexagonally arranged nanodot arrays. Alloy nanodot arrays with precisely defined element ratio were also able to be synthesized, which was usually a significant challenge in solution-based fabrication technologies. The fabricated surface patterns exhibited interesting optical

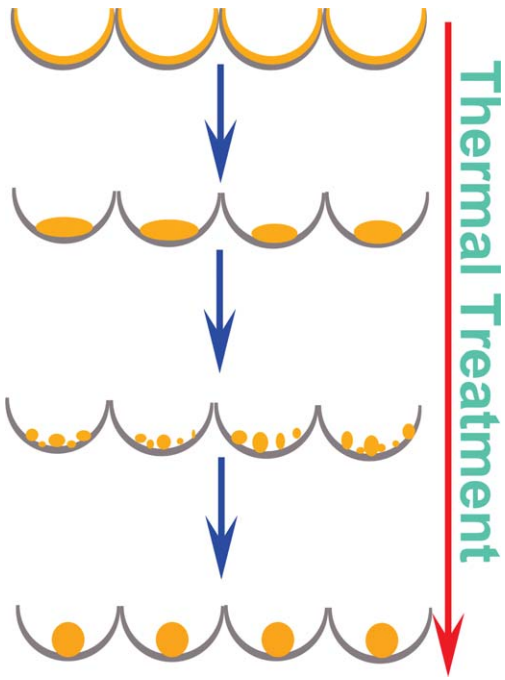

Scheme 3 Schematic illustration for the fabrication of metallic surface nano-patterns by template confined dewetting approach. The grey and golden colors represent the silica and gold.

properties, such as strong near infrared light absorption and high SERS performances.[39] With similar bowl template formed with alumina instead of silica to do electrochemical deposition of gold, highly surface roughened gold particle arrays could be prepared. Such prepared gold particle arrays showed strong SERS enhancement.[40]

4.2 Nanopillars

In the past few years, 1D nanostructures (metals, oxides, and carbides) have been fabricated by various methods. And these 1D nanostructures have shown applications in solar cells, sensors, transistors and battery electrodes.[41–43] Ordered 1D nanostructures arrays can optimize their property performances drastically such as in photonic and battery application areas.[44,45] Hexagonally arranged 1D nanostructure can be grown from the MCC templates using the outstanding GLAD approach. By this route, various nanopillar arrays have been prepared.[46,47] Fig. 5a shows the representative Si nanopillar arrays obtained by this methodology.[46] Similarly, by performing pulsed laser deposition (PLD) on the MCC template, hexagonally located nanopillar arrays of diverse materials were realized.[48–52] The formation mechanism of these nanopillar arrays were schematically shown in Fig. 6. Subsequently, the wetability, field emission, catalysis performances of the hexagonally arranged nanopillar arrays were investigated. Fig. 5b and 5c give the typical top and side view of the close packed TiO_2 nanopillar arrays. Interestingly, the nanopillar array could be further transferred to another arbitrary substrate allowing for the fabrication of nanopillar arrays on the desired substrates for various device applications (especially on flexible substrates such as plastic plates, which is important in flexible device fabrications). The as-fabricated nanopillar arrays demonstrated superamphiphilicity with both water and oil contact angles of 0°, without ultra-violent light exposure. Moreover, the synthesized amorphous TiO_2 nanopillar array exhibited better photocatalytic performance than the anatase nanopillar array due to its large surface area and special microstructure. Self-cleaning surface could be realized based on the nanopillar arrays which showed both excellent photocatalytic and superamphilphilicity activity.[48] Also, non-close-packed TiO_2 nanopillar arrays could be prepared by heating the as-fabricated nanopillar arrays at 650 °C for 2 h.[49] Other materials such as hematite and Co_3O_4 hierarchical columnar arrays could also be fabricated with this protocol, as shown in Fig. 5d. These columnar arrays also exhibited novel wettability phenomena. Qi *et al.* adopted a quite different way to get hexagonally arranged nanorod arrays. First, the bowl template was derived from the MCC template by the silica sol infiltration.[32] Then, ZnO nanopillars were preferentially grown at specific sites (*i.e.*, the bottom of the bowls) on a zinc foil through a wet chemical method. Consequently, hexagonally patterned arrays of

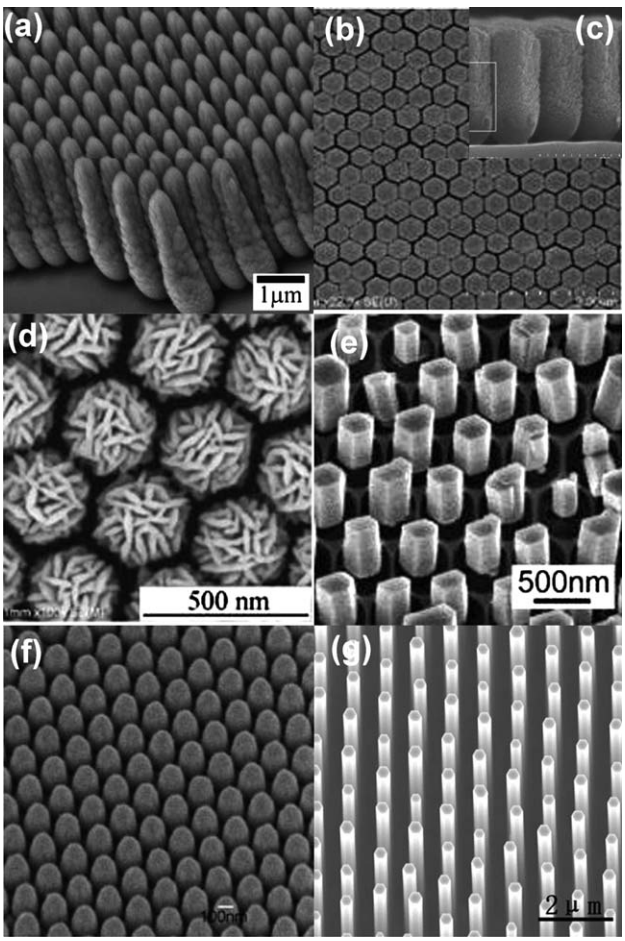

Fig. 5 Hexagonally arranged nanopillar arrays depending on the MCC template. (a) Si nanopillar array fabricated by GLAD. (b) and (c) Top and side view of the TiO_2 nanopillar array synthesized by pulsed laser deposition. (d) Hematite nanopillar array obtained by pulsed laser deposition. (e) ZnO nanopillar array acquired by a wet chemical deposition with the bowl template derived from the MCC template. (f) Silica nanopillar array synthesized through reactive ion etching using MCC templates as masks. (g) ZnO nanopillar array made from physical vapour deposition with hexagonally arranged gold nanoparticles as catalysts. ((a) ref. 36, (b) to (d) ref. 38, (e) ref. 41, (f) ref. 43, (g) ref. 45.)

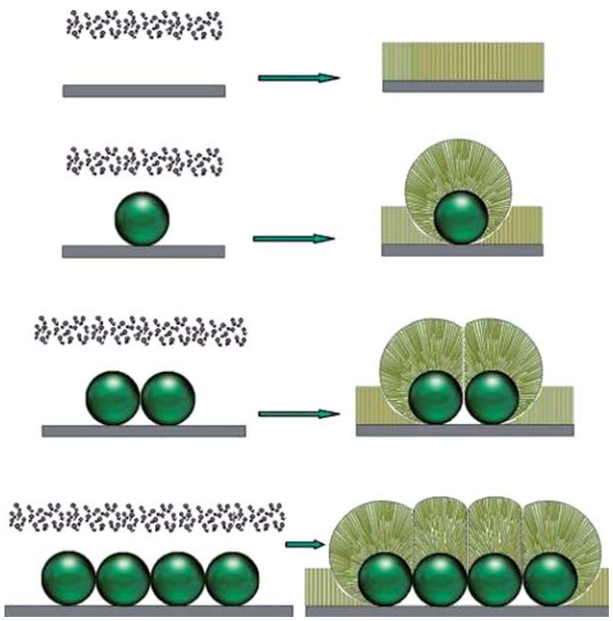

Fig. 6 Schematic illustration of the formation process of the TiO_2 nanopillar array by pulsed laser deposition on the surface of the MCC template.[38]

well-aligned ZnO nanopillars were obtained (Fig. 5e). The size, morphology, and orientation of the nanopillars could be adjusted by changing the experimental parameters.[32] Reactive ion etching (RIE) was also used to treat silica substrates covered by MCC templates.[53] After such treatment, silica nanocone arrays were prepared (Fig. 5f). Importantly, such surfaces dramatically suppressed reflection over a wide range of light. Thus it is possible to use these structures in display, projection optics, laser and laparoscopic surgery application areas. Also, such antireflection surfaces showed superhydrophilic properties. This RIE method was extended in the fabrication of silicon nanocone arrays.[54] The wettability behaviour of the synthesized nanocore arrays was investigated in details. A novel route to synthesize highly ordered ZnO nanopillar arrays was also studied based on the MCC template.[55] A thin layer of gold membrane was first evaporated on a substrate. Subsequently, a MCC template was assembled on the gold surface. Plasma etching was performed to remove the gold species and left the gold film at the areas where protected by the PS spheres. After removing the PS spheres, hexagonally arranged gold nanodot arrays came forth. Well ordered ZnO nanopillar array could be fabricated by chemical vapour deposition with the as-prepared hexagonally situated nanoparticles as catalysts (Fig. 5g).[55]

4.3 Hollow spheres

Hollow nanostructures have received significant research attention due to their large surfaces and hollow structures. They can be used in a wide application regions, such as catalysis, drug release, energy-related areas, and so forth.[56–60] MCC templates have been widely harnessed in the fabrication of hollow sphere arrays.[61–65] The representative method is *via* electrochemical deposition on the surface of MCC template.[61–63] After removing the plastic spheres, hollow sphere arrays are realized. The key step in the realization of the deposition of materials on the surface of the PS spheres is the introduction of a seed layer.[61,62] Without such a seed layer, materials will preferentially be deposited on the substrate, instead of on the surface of PS spheres.[31] By introduction of a thin layer of gold film on the MCC template, various hollow sphere arrays were prepared ranging from metals (*e.g.*, Au, Fig. 7a) to semiconductors (*e.g.*, CdS) and further to organic materials (*e.g.*, polypyrrole).[61] Through first immersion of the MCC template in concentrated $ZnCl_2$ aqueous solutions, and then conducting electrochemical deposition of ZnO, hollow urchin-like ZnO spheres were prepared (Fig. 7b). This is a simple and low-cost method to prepare highly ordered ZnO hollow sphere arrays, which has potential applications in optical devices, photonic crystals, and nanodevices.[62] Ni hollow sphere arrays can also be prepared through this method.[63] Electrophoretic deposition method has become a mature way to fabricate coatings on surfaces. We found that hollow sphere arrays can also be synthesized by the electrophoretic deposition on the MCC template surfaces in the colloidal solutions. Si and Ag hierarchical hollow sphere arrays were prepared as shown in Fig. 7c and 7d.[64,65] The structural parameters, including the size, shell thickness, feature of the nanoshells and the inter-shell spacings, can be tuned conveniently. The influence of these parameters on the optical properties of the Ag nanoshell array was studied in details. They can support multiple surface plasmon resonances and show strong SERS enhancement, which will be introduced in section 6.

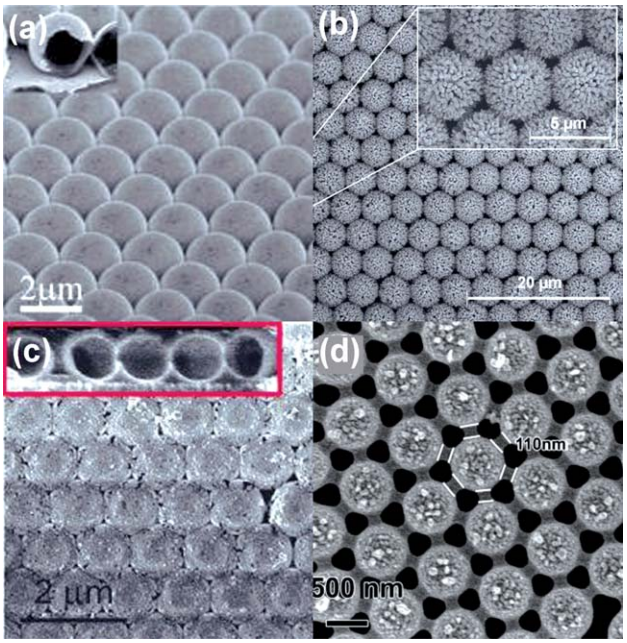

Fig. 7 Hollow sphere arrays obtained by the MCC template. (a) Gold hollow sphere array synthesized from electrochemical deposition on the seeded MCC template. (b) ZnO urchin-like hollow spheres fabricated by electrochemical deposition. (c) and (d) close packed Si hollow sphere array and non-close packed Ag hollow sphere array prepared by electrophoretic deposition on the MCC template. ((a) ref. 51, (b) ref. 52.)

4.4 Bowls

Nanometre-scale bowls can be used as micro-reactors and containers. Obviously, there are two ways to generate bowl arrays depending on the MCC template. The first one is through etching the hollow spheres into bowls. The second and more straightforward route is to selectively grow materials on the top or bottom surface of the PS spheres. In consequence, after removing the PS spheres, bowl arrays can be generated. TiO_2 bowl arrays have been fabricated through ion milling of the hollow sphere array synthesized by atomic layer deposition route (Fig. 8a).[66] Furthermore, such prepared bowl arrays can be used as a mask to fabricate small nanodot arrays. As is well-known, during thermal evaporation, materials will be deposited on the upper surface of the PS spheres in the MCC template due to the shadow effect. The optical properties of the Ag bowl arrays fabricated by the thermal evaporation have been studied.[67] The inter-bowl distance could be controlled by the plasma pretreatment of the MCC template. The correlation between the SERS enhancement and the nanoscale features was studied. It was found that both the local surface plasmon mode and the delocalized surface plasmon resonances contributed to the SERS enhancement.[57] The plasmonic properties of the Ag bowl arrays were further studied by Li and his coworkers.[68] The plasmonic properties could be tailored by changing the inter-bowl distances. The bowl arrays were good candidates in sensor applications, especially in label-free, real-time biosensors to detect

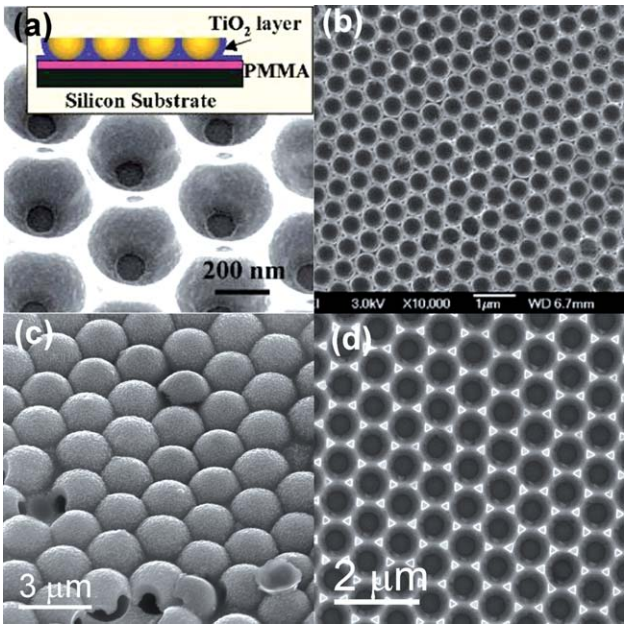

Fig. 8 Bowl arrays prepared *via* the MCC templates. (a) TiO_2 bowl array fabricated by ion milling of the TiO_2 hollow spheres. Inset gives the schematic synthesis protocol. (b) Ag bowl array from evaporation on the MCC template. (c) MnO_2 microcap array obtained from seed-mediated electrochemical deposition. (d) MnO_2 bowl array realized by electrochemical deposition. ((a) ref. 56, (b) ref. 59.)

biomacro-molecules.[58] Such prepared bowl arrays could be turned over by adhesive tapes as shown in Fig. 8b.[69] The bowl surface was formed with Ag nanoparticles with sizes around 10 nm, allowing them to be good candidates in SERS and catalysis.[69] Very recently, we found that the evaporated thin layer of Ag film on the top half surface of the PS spheres could be used as a seed layer to grow other materials, such as Pt, Cu, MnO_2, PANI and Au. This means that the nucleation place on the PS spheres in the MCC template can be controlled during the electrochemical deposition process. Therefore, a versatile technique to fabricate various bowl arrays including Pt, Ag, Cu, MnO_2 and PANI (polyanine) was designed and schematically shown in Scheme 4. The representative microcap array of MnO_2 fabricated by the seed-initiated electrochemical deposition method was shown in Fig. 8c.[70] Notably, such fabricated microcap arrays were freestanding and could be transferred onto other arbitrary substrates. Also, inversion of the microcap arrays could be realized and changed into bowl arrays.[70] A facial chemical route to synthesize Ag hierarchical bowl arrays based on the MCC template was also presented. In the method, a silver acetate solution was dipped on the surface of the MCC template. After subsequent heating decomposition, Ag bowl arrays were obtained.[71] A powerful approach to synthesize freestanding bowl arrays at the gas/liquid interface was developed recently. At the beginning, MCC templates were transferred on the surface of suitable precursor solutions containing $HAuCl_4$ and Na_2SO_3. Subsequently, the whole system was exposed under the ultraviolet light. After 12 h ultraviolet light irradiation and then removing the PS spheres, gold bowl arrays were formed.[72] Electrochemical deposition could also be used in the fabrication of bowl arrays using MCC templates. During the deposition process, species will be filled in the interstitials among the three adjacent PS spheres. After dissolving the PS spheres, bowl arrays could be acquired. Very recently, based on this methodology, we successfully fabricated bowl arrays of MnO_2, which might show good performances in supercapacitors and rechargeable lithium ion batteries (Fig. 8d).

4.5 Nanorings

Nanoring arrays have applications in areas ranging from microelectronics, optoelectronics, magnetic storage, and sensors.[73–75] A wet chemical approach was adopted for the preparation of large area metal nanoring arrays.[76] Briefly, metal precursors were reduced in the interstices between the MCC template and the substrate. After removing the PS spheres, platinum, gold and copper nanorings were fabricated.[76] Fig. 9a shows the fabricated platinum nanoring arrays. An efficient and universal strategy for the nanoring array preparations was developed by Sun and his coworkers.[77] Large area arrays of PS, magnetite, gold, silicon, magnetite nanoparticle/PS and gold/PS composite nanorings were obtained (Fig. 9b). Importantly, these nanorings could be detached from the substrate and become freestanding nanorings in the liquid, which might be used in bio- and chemical sensors.[77]

4.6 Nanocrescents

The plasmonic properties of the metallic nanostructures are highly dependent on the morphology and the interactions between neighbouring units. Therefore, adjusting the shape of the metallic nanostructures is important in plasmonic

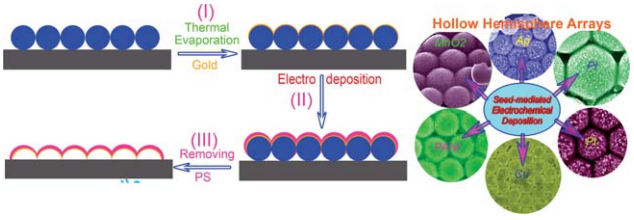

Scheme 4 Schematic illustration for the fabrication of hollow hemisphere arrays depending on the seed-mediated electrochemical deposition methodology. The right image shows various hollow hemisphere arrays prepared.

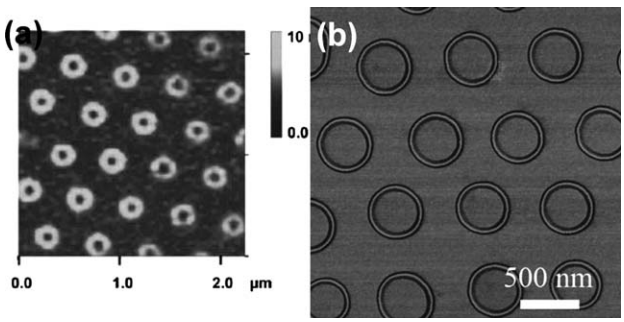

Fig. 9 Nanoring array of platinum (a) and PS (b). ((a) ref. 66, (b) ref. 67.)

regions.[78,79] The sharp edges in the nanocrescent will enhance local electromagnetic field dramatically, which is crucial in SERS applications. By the combination of conventional film deposition method and the MCC template, gold nanocrescent arrays were prepared.[80] Unique multiple surface plasmon resonances were observed in a single nanocrescent. The SERS enhancement of the nanocrescent could reach as high as 10^{10} order. This is very attractive in ultrasensitive detections of biomolecules. The optical properties of the gold nanocrescent was further studied. It was found that the plasmon-induced electromagnetic near-field around gold nanocrescent antennas exhibited localized surface plasmon bands in the infrared.[81,82] By analogous fabrication methodology, three dimentional gold-nanocrescent resonators were fabricated (Fig. 10).[83] The interactions between neighbouring gold crescent provided interesting optical properties. High-quality optical metamaterials can be anticipated based on the three dimensional gold nanocrescent arrays.[83]

4.7 Pores

Atomic layer deposition was harnessed to synthesize pore arrays of SiNx (Fig. 11a).[84] By constructing the arrays of high refractive index materials SiNx on various phosphor membranes such as Y_2O_3:Er^{3+}, the photoluminescence was enhanced by up to one order of magnitude. This method could realize wafer-scale fabrications of various pore arrays, which is highly desirable for applications in the mass production of photonic, optoelectronic and sensor devices.[84] Freestanding nanonets (*i.e.* pore array) can be fabricated at the gas/liquid interface.[85] First, MCC templates were formed on the surface of various salt solutions (*e.g.*, $AgNO_3$). Then reactive gas (*e.g.*, H_2S) was introduced into the system. H_2S gas will pass through the MCC template and react with $AgNO_3$, leading to the formation of AgS_2 precipitates at the gas/liquid interface. After dissolving the PS spheres, AgS_2 nanonets were obtained (Fig. 11b).[85] This method could also be extended to prepare other freestanding nanonets. During electrochemical deposition on the MCC template, we found that silver pore arrays could be prepared after dissolving the PS spheres (Fig. 11c). Interestingly, the skeleton composed of small sized Ag nanoplates, which will have potential applications in plasmonics, sensing and SERS areas.[86] The related works are still under process.

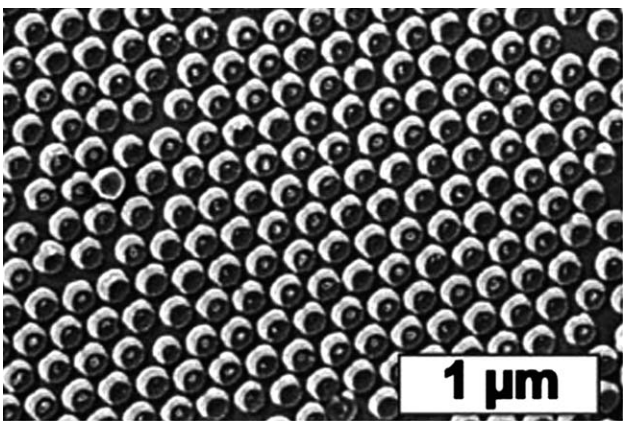

Fig. 10 SEM image of the nanocrescent array (ref. 73).

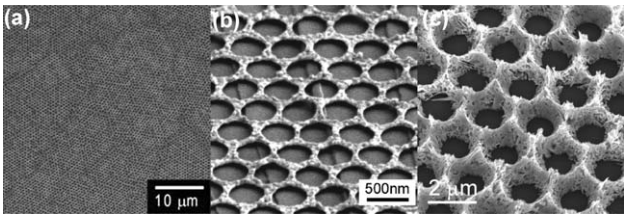

Fig. 11 (a) SiNx pore array synthesized by atomic layer deposition; (b) AgS_2 freestanding pore array acquired at the gas/liquid interface; (c) Ag pore array fabricated by electrochemical deposition. ((a) ref. 74, (b) ref. 75.)

5. Non-close-packed MCC template-induced surface patterns

As mentioned above, the existence of a small spacing between building blocks in the ordered array is sometimes important in special application dormitories such as in SERS and field emissions. Non-close-packed (ncp) MCC templates can meet these requirements to some degree. Ncp MCC templates can be fabricated by etching on the MCC templates.[87] The spacing between the adjacent PS spheres in the ncp MCC template can be tailored by controlling the etching time. Simultaneously, the sizes of the PS spheres are decreasing during the etching process. Various etching methods including ion polishing, reactive ion etching and plasma etching are used to reduce the sphere diameters in the MCC template. An isotropic etching and the position fixing of the PS spheres during the etching process are crucial in realizing the ncp MCC template. Plasma etching is an isotropic etching process for PS spheres.[88] In order to maintain the position of the PS spheres during the etching process, pre-heating of the MCC template (*e.g.*, 110 °C for 10 min) is indispensable.[89] The ncp MCC template can be adopted to fabricate cylindrical holes with hole-to-hole distance controllability by thermal evaporating metallic materials on the surface of the template (Scheme 5).[89] Ni ordered porous arrays acquired by this method exhibit significantly higher coercive force and remnant magnetism than those of the continuous films without the cylindrical holes, indicating that these Ni porous films should be useful in the next generation of nano-devices for data storage and sensing.[89] The optical responses of the hybrid photonic-plasmonic crystals can be tuned by filling the dielectric species into the ncp MCC template.[90] It was found that a small decrease of filling fraction of the lattice leads to prominent spectral blue-shifts and variations on the spatial distribution of the total field intensity depending on the character of the mode investigated.[90] Highly ordered Si nanowire arrays were prepared by the ncp MCC template according to the following protocols. First, a MCC template was fabrication on a piece of Si wafer followed by the etching transformation to a ncp MCC template. Then a thin layer of silver film was evaporated (Scheme 5). Finally, the Si wafer capped by porous silver film was immersed in the aqueous solution containing HF and H_2O_2. The Ag film can facilitate the etching of the beneath Si wafer, leading to the formation of ordered Si nanowires.[91] Using this method, Si-Ge hetero-structured nanowires can also be synthesized.[91] Besides the metal-assisted etching toward the fabrication of Si nanowires, ncp MCC templates can be used directly as masks during

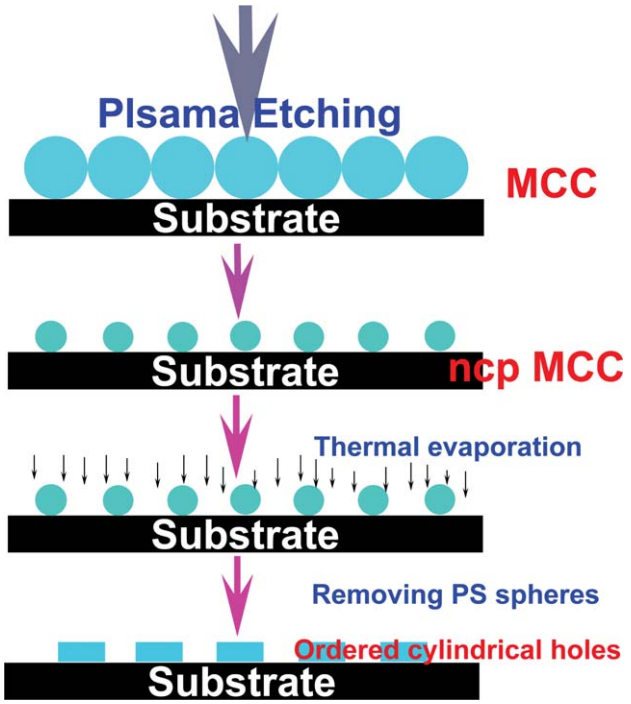

Scheme 5 Schematic demonstrated for the synthesis of ordered cylindrical holes depending on the ncp MCC template.

the reactive ion etching treatment of Si wafers.[92] By thermal evaporating silver on the ncp MCC template, silver half-shells have been fabricated and the relations between the SERS performance and the shell-shell distances are studied.[67] Also the plasmonic properties are highly related to the shell-shell spacings.[67] These facts underlie that the silver shell-to-shell spacing adjustment is important in the sensing applications, *i.e.*, the spacing manipulation between PS spheres in the ncp MCC template is substantially important. Biological related surface nanopatterns are powerful platforms to address some fundamental issues, including protein-protein and cell-protein interactions. The ncp MCC template can also be used in the fabrication of protein surface nanopatterns.[93]

Obviously, the diameter of the spheres and the inter-sphere spacing of the ncp MCC template prepared by plasma etching are highly dependent on the diameter of the PS spheres in the starting close-packed MCC template. In some cases, independent adjustment of the size and the spacing between the PS spheres in the template is desired. Therefore, an alternative way has been developed to prepare the ncp MCC template, which depends on the self-organization of the charged spheres at air/water or oil/water interfaces. The existence of the electrostatic repulsion and capillary attraction between neighboring hydrophobic spheres will induce the formation of ncp MCC template.[94] The variation of the surface pressure of the sphere film at the air/water or oil/water interface enables the controlling of the inter-sphere distance in the ncp MCC template. Also, an external electric field can be applied in order to acquire larger area homogeneous patterns.[94] Although uniformly structured patterns can be obtained at ease at the air/water or water/oil interfaces, transferring them on a substrate becomes a difficult and critical step. Sufficient care should be taken during the transferring step and otherwise the well-defined structure will be destroyed. In order to keep the pattern structure during the transferring process, several requirements are needed. The first one is that strong attractive forces should be created between the spheres and a substrate for anchoring the isolated spheres on the substrate. This can be realized by modifying the substrate to have an opposite charge to that of the sphere surface.[94] A second requirement is that capillary forces should be reduced during the drying process of the pattern after transferring on a substrate. Otherwise, the pattern structure might be disrupted, especially for micrometre-sized sphere-formed MCC template. The capillary forces can be reduced by solvent exchange prior to drying.[94] After transferring the patterns on the substrate, they can be used as templates to synthesize surface nanopatterns as shown in Scheme 1. The synthesized surface patterns have different applications in biosensing and antireflective coatings.[94]

6. Properties and device applications

6.1 Sensing devices

Because the metallic surface patterns are sensitive to the nature of the surrounding medium (*e.g.*, dielectric variations), they are widely used in label-free sensing of chemicals. For example, the nanocrescent shows high sensitivity of dielectric colloids.[95] The nanocrescent arrays are potential candidates as label-free and real-time bio-sensors. The honeycomb arrays of metallic triangulars have been investigated to be used as reusable and stable bio-oriented sensors. A layer of silica matrix was used to cap the honeycomb array to enhance the stability (Fig. 12a).[96] The reusability of the substrate could be clearly seen in Fig. 12b.[95] The nanocrescent could be used not only as LSPR based sensors, but also be harnessed in SERS sensing. The enhancement factor can reach 10^{10} for a single crescent.[80] Silver nanoshell (hollow sphere) arrays were also candidates in the LSPR based sensing criteria, due to the multiple LSPS peaks existed. Besides this, the Ag nanoshell arrays are good SERS substrates with reproducible and strong SERS enhancement.[65] The correlation between the nanoshell structures and the SERS enhancement factors are systematically studied by us. As shown in Fig. 12c, as the spacing between the neighboring nanoshells decreased, the SERS enhancement factor increased. On the other hand, the feature of the nanoshell would also affect the SERS enhancement. Free-standing Ag porous film was prepared at the gas/liquid interface, which was also a good SERS sensor candidate substrate.[97] Besides these optical-related sensors, pore arrays of In_2O_3 and SnO_2 have been explored in gas sensing applications.[98–100] The MCC template was transferred on the precursor solution firstly, and then the MCC template with a little amount of precursor solution was picked up by a ceramic tube. Consequently, another layer of MCC template (with different PS diameter) was enwrapped on the same ceramic tube by the same protocol as shown in Fig. 13a.[98] After burning the PS spheres, double layered pore array could be prepared (Fig. 13b). This is a flexible way to synthesize pore arrays with different parameters (*e.g.*, pore size, roughness of the skeleton). The synthesized In_2O_3 pore array demonstrated both higher sensitivity and much faster response to NH_3 gas than the corresponding conventional In_2O_3 intact film. The performance of the gas sensors could be manipulated by the

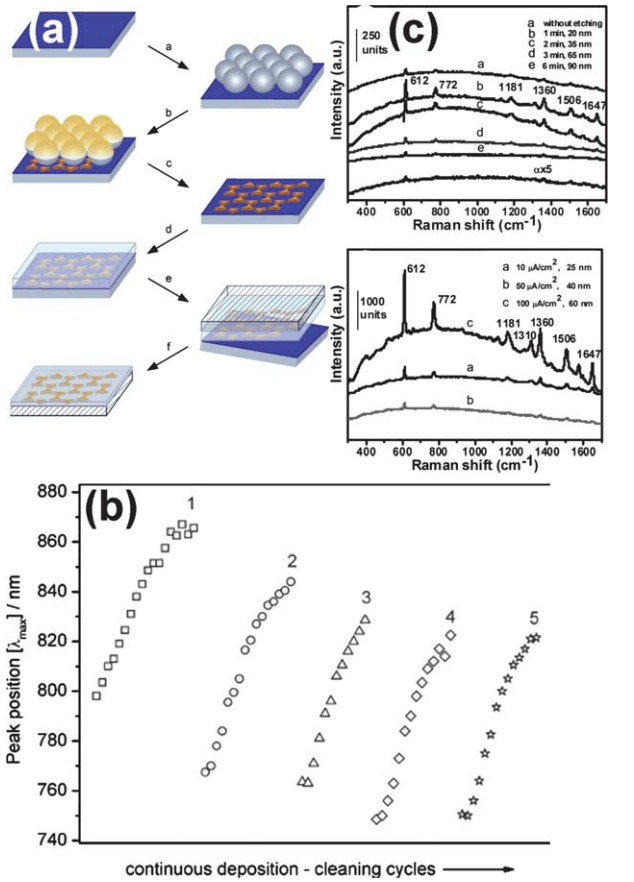

Fig. 12 (a) Schematic illustration for the preparation of the honeycomb array enclosed by silica matrix; (b) the reusability evaluation of the substrate: (c) SERS enhancement of the Ag nanoshell array. ((a) and (b) ref. 78.)

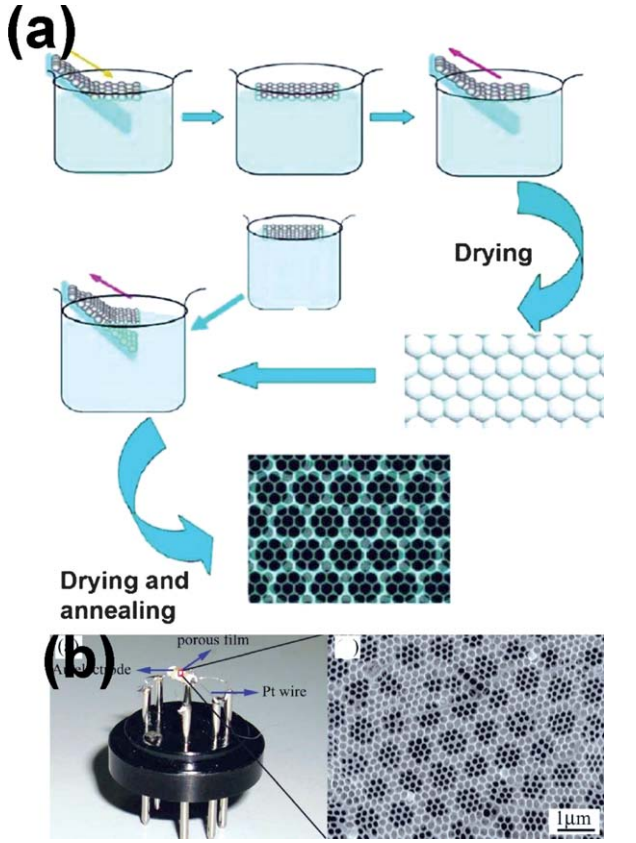

Fig. 13 (a) Schematic illustration of the fabrication process of the porous films on the ceramic tube; (b) gas sensor device (left image) and the corresponding SEM image of the porous film (ref. 80).

pore size of different layers. This work shed new light on real gas sensing applications of porous films.[97] This method can also be used to fabricate SnO_2 pore arrays. Interestingly, the doping of metal ions will influence the sensitivity of the gas sensor devices prominently. When the doping amount was 1% M, the Cr^{3+} and Pd^{2+} doped pore arrays demonstrated a dramatically enhanced sensitivity and strong selectivity to ethanol and ammonia, respectively.[100]

6.2 Energy-related applications

Rechargeable lithium ion batteries have received much investigation interest in recent years. The electrode material will determine the performance of the batteries, such as the capacity and the cycling properties. Various materials have been explored as the electrode candidates. Cobalt oxide bowl arrays were prepared by electrochemical deposition using the MCC template as electrode.[101] There were many individual pores of about 50 nm on the surface of the micrometre sized bowls. The interstices between adjacent bowls were filled by small cobalt oxide flakes. It was found that the annealing treatment will change the electrochromism properties. The bowl array treated under 200 °C exhibited good electrochromism with color changes from dark gray to pale yellow and fast response time. These as-prepared cobalt oxide bowl arrays were further explored as the electrode in lithium ion batteries, which might supply a good electrode candidate.[101] Nickel oxide bowl array was fabricated by similar technique.[102] The morphology was also resemblance to that of the cobalt oxide. When the nickel oxide bowl arrays were harnessed as the anode material for lithium ion batteries, they showed weaker polarization, higher coulombic efficiency and better cycling properties in comparison with the nanoparticle films.[102] Similarly, nickel phosphide bowl arrays were prepared and investigated as electrodes in lithium ion batteries.[103] MCC templates on the Si wafer could be changed into ncp ones by plasma etching, as discussed in Section 5. A thin layer of silver film was thermally deposited on the ncp MCC template. Then, the substrate was immersed in the mixture of HF and H_2O_2 aqueous solution. Finally, highly ordered Si nanopillar arrays were acquired (Fig. 14b).[104] The surface had excellent antireflection property with a low reflection loss for the incident light within the visible light range. The solar cell formed by the antireflective Si nanopillar array (Fig. 14a) showed power conversion efficiency of about 9% with a short circuit current density of about 29.5 mA cm^{-2} (Fig. 14c and 14d).[104] Electrolysis of a special precursor solution was used to synthesize titanium oxide hollow sphere arrays depending on the MCC templates.[105] The titanium oxide hollow sphere arrays could be used in dye-sensitized solar cells, exhibiting higher energy-conversion efficiency than the corresponding nanoparticle film electrode.[105] The

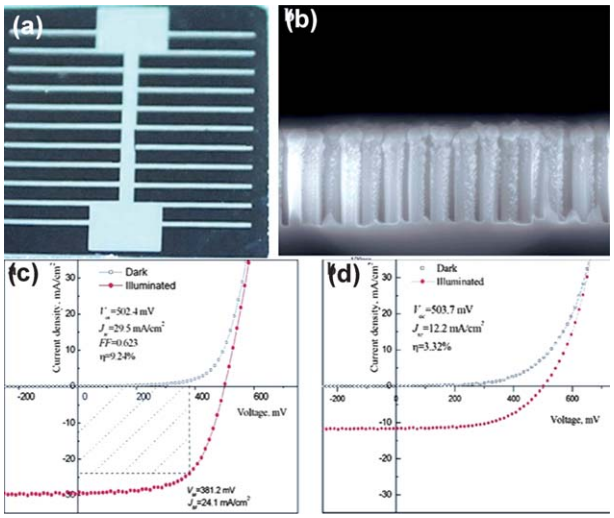

Fig. 14 (a) Photograph of the solar cell formed by Si nanopillar array; (b) SEM image of the Si nanopillar array; (c) and (d) are *J–V* curves of the solar cells composed of (a) and without (b) the Si nanopillar arrays in darkness and under AM 1.5 G illumination (ref. 86).

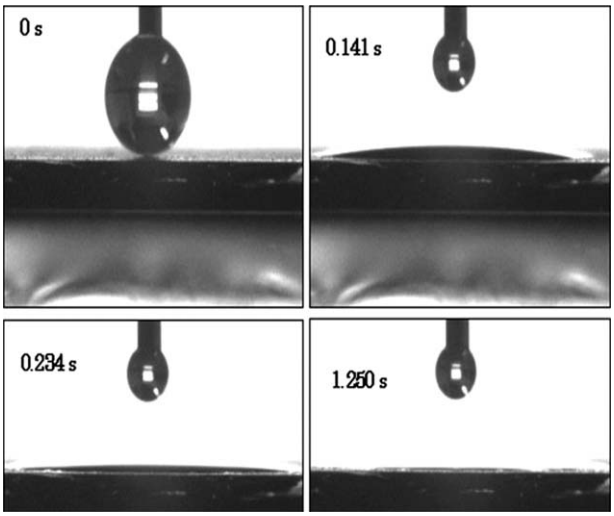

Fig. 15 The process of the water contacting behaviour on the surface of the TiO2 nanopillar array (ref. 40).

MnO_2 bowl arrays shown in Section 4.4 will have potential applications in supercapacitors, which is now under investigations in our group.

6.3 Wetting behaviour

The wetting behavior of a solid surface has important and wide applications in self-cleaning, micro-fluidics, and antifogging coatings.[106–108] Therefore, controlling the wetting behaviour of a surface becomes a hot topic in materials science and engineering areas. Ordered nanopillar arrays of Co_3O_4, hematite, and TiO_2 synthesized by pulsed laser deposition on MCC templates show fascinating wetting behaviors.[48–52] These nanopillar arrays have superhydrophilicity without ultraviolet irradiation, which are ascribed to the improved roughness and the existence of a large amount of OH^- groups.[48–52] After chemical passivation with fluorosilane on the Co_3O_4 nanopillar arrays, the superhydrophilicity could be tuned to superhydrophobicity.[52] The TiO_2 nanopillar arrays demonstrate excellent superhydrophilicity with a water contact angle of 0° without ultraviolet irradiation, as shown in Fig. 15. The wetting behaviour is very stable and could be maintained for several months, having big application potentialities in self-cleaning surfaces and microfluidic devices.[50] The silicon nanopillar arrays fabricated by metal-catalysed etching of silicon wafer using MCC templates show water repellent properties without any modifications.[108]

6.4 Field emitters

Field emission of semiconductor nanostructures is crucial in the application areas including integrated circuits, flat-panel displays, microwave power amplifiers, and other microelectronic devices.[109–112] Amorphous silicon nanopillar arrays were synthesized by reactive ion etching of Si wafers (capped by 70 nm amorphous silicon layer) using the MCC templates as masks.[113] A low turn-on electrical field of about 4.5 V μm^{-1} at a current density of 10 $\mu A\ cm^{-2}$ and a high current density (>0.2 mA cm^{-2}) at 9 V μm^{-1} were observed. The field enhancement factor could reach 1240 calculated by the Fowler-Nordheim relationship.[113] TiO_2 nanopillar arrays fabricated by pulsed laser deposition on the MCC templates were amorphous. During the crystallization process (heating treatment), the volume of the nanopillar shrank, leading to the formation of ncp nanopillar arrays.[49] The merit of this fabrication technique is that the structural controlling can be easily realized, which makes it possible to design field emitters with optimal performances.[49] Experimental results show that nanopillar arrays with a smaller periodicity and a broader spacing have the best field emission performance.[49] Honeycomb array of ZnO nanorods synthesized by electrochemical deposition in the interstitals of the shape-deformated MCC templates were fascinating field emission material candidates (Fig. 16).[31] The nanorod density, uniformity, and tapering could be manipulated by experimental parameters. The diameter of the PS spheres in the MCC templates will influence the field emission properties, as shown in Fig. 16. As the sphere diameter decreased from 1000 nm to 500 nm, the turn-on fields decreased prominently. However, it slightly increased when the sphere diameter further decreased.[31] After experimental optimization, a low turn-on electric field of 1.8 V μm^{-1}, a high emitting current density of about 2.5 mA cm^{-2}, and a field enhancement factor of 5750 were achieved. These ZnO nanorod array could be used in cold-cathode-based electronics.[31]

6.5 Antireflection

In nature, some insects can use non-close-packed protrusions to enhance the light transmission, improving their vision in darkness. In real applications, decreasing the reflection and enhancing the transmission of light are of prime importance in optical and electro-optical devices.[114] By mimicking the structure of the cornea of moth, silica antireflection surfaces were prepared (Fig. 6f). The reflection and transmission spectra were detected for evaluation the antireflection property (Fig. 17).[53] The reflection of the silica nanorod arrays (double-side) was smaller than 2% over a wide wavelength range from 300 to 800 nm (the grey

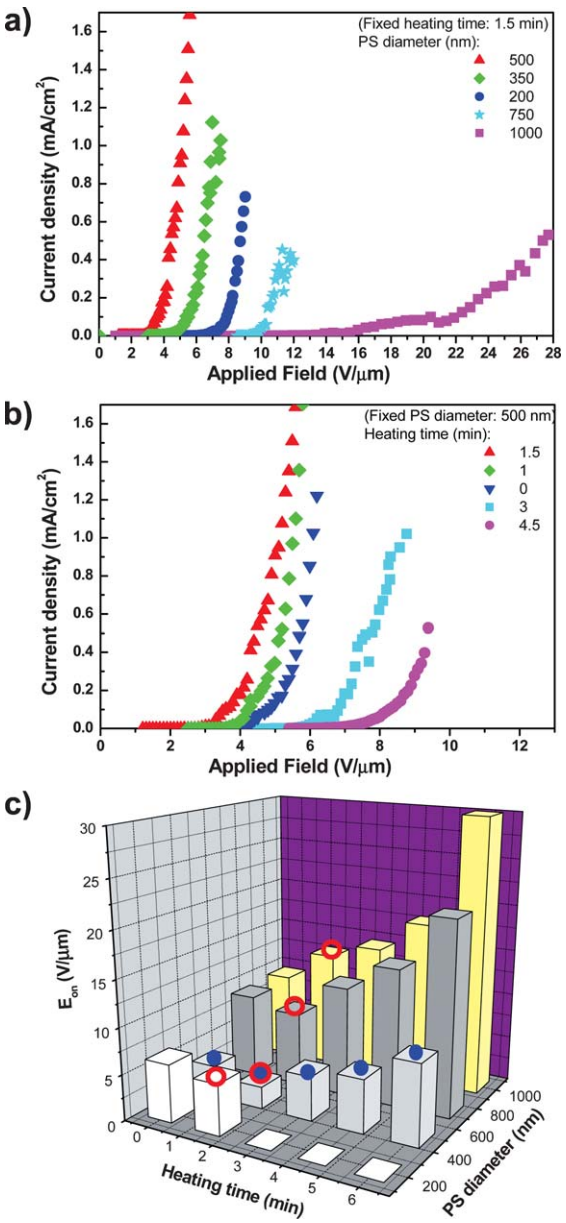

Fig. 16 *J–E* curves of ZnO nanorod array anodes with different sized PS spheres (a) and different heating times (b). (c) Summarized dependence of turn-on electric field on PS diameter and PS heating time (ref. 26).

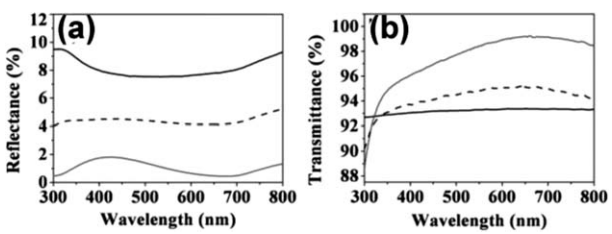

Fig. 17 The performance of the antireflective properties. (a) comparison of the reflection of a planar silica surface (black line), single-sided (black dash line) and double-sided silica nanopillar array (grey line). (b) Wavelength-dependent transmission of planar silica surface (black line), single-sided (black dash line) and double-sided silica nanopillar array surfaces (grey line) (ref. 43).

line in Fig. 17a). However, the value exceeded 8% for planar silica glass (the black line in Fig. 17a).[53] Accordingly, the transmission of the former surface was larger than 99% from 610 nm to 700 nm (the grey line in Fig. 17b), whereas the latter surface was smaller than 93% (the black line in Fig. 17b).[53] According to theory calculations, the antireflective performance of a surface was strongly dependent on the aspect ratio of the building units in the array. High aspect ratio of silicon hollow-tip arrays were also fabricated by the MCC templates.[115] A silver membrane was first thermal evaporated on a silicon wafer surface using the ncp MCC template as a mask. Then metal-catalysed route was used to manufacture the silicon wafer surface. Subsequently, the synthesized silicon nanorod array were tapered by reactive ion etching. Finally, silicon hollow-tip arrays were obtained. It was found that the silicon hollow-tip arrays can suppress the light reflection in the wavelength region ranging from the ultraviolet to the mid-infrared. Lower than 1% reflectance was achieved in the 250 to 1600 nm range for the optimized sample. Such surfaces have promising applications in improving the energy conversion efficiency of solar cells.[116] Large scale ordered Y_2O_3:Er^{3+} porous films were synthesized using the MCC template. The fabricated membrane shows bifunctionality and broadband antiflection in the wavelength ranging from 300 nm to 1100 nm. Also, it exhibits strong red and infrared light emissions under 1538 nm excitation.[117]

7. Summary and outlook

In this review, we have summarized recent developments of the surface patterning techniques based on the MCC and ncp MCC templates. Various surface patterns have been fabricated through the MCC surface patterning techniques, including hexagonally arranged arrays and honeycomb arrays. The building units of the ordered arrays include nanodots, nanopillars, nanorings, nanodisks, pores, hollow spheres, bowls, and others. Various deposition techniques, such as thermal and sputtering evaporation, pulsed laser deposition, atomic layer deposition, GLAD, electrochemical and electrophoretic deposition are adopted in the surface patterning processes depending on the MCC templates. The structural control of the surface patterns can be realized easily. High through-put and low-cost production of ordered arrays of surface patterns with high structural uniformity can be achieved. The developed surface patterning synthesis routes motivated the device applications of the surface patterns in various areas, such as in sensing devices, energy-related areas, wettability-control regions, field emission fields, and antireflection domains.

For the future work regarding the fabrication of the MCC templates, the preparation of large-scale ordered MCC template without defects is still a big challenge. New methods that could reduce the possibility of the appearance of defects during the self-assembly process of PS spheres are highly needed. This is a crucial step to make the PS spheres a competitive and promising MCC template in the surface patterning fields. In addition, so far it is very hard to assemble PS spheres with sizes less than 100 nm. Novel techniques to synthesize MCC templates composed of small PS spheres (<100 nm) are highly desirable, which is of prime importance to realize surface nanoscale patterns. As to the synthesis of surface patterns, fabrications of

complex surface patterns are necessary in the future. Surface patterns with geometrical structures other than the aforementioned honeycomb and hexagonally arranged arrays will have important applications in some special devices. Hybrid materials formed surface patterns should be explored on the basis of the metallic, metal oxide, and metal sulfide surface patterns, which will supply more interesting properties and application potentials. Multiple layered surface pattern synthesis is still lack of investigations, which should be able to be acquired through a layer-by-layer route. These multiple layered structures will show interesting optical properties. Interesting metamaterials might be fabricated by a low-cost method based on the MCC template. Moreover, layered devices are anticipated with excellent performances, such as supercapacitors and lithium ion batteries. Exploration of the surface pattern synthesis on flexible substrate is also interesting and it may lead to the formation of flexible devices based on the MCC template, such as flexible light emitting diodes. Moreover, the investigation of the applications of the surface patterns synthesized by the MCC templates may be able to be widened into bio-related areas, due to their micrometre scale building blocks. As a relative new surface pattern fabrication technique depending on the MCC template, it will become a powerful alternative tool in surface patterning synthesis in addition to the other conventional fabrication methodologies.

Acknowledgements

Financial support from European Research Council Grant (ThreeDSurface) is gratefully acknowledged.

References

1 J.-W. Jang, Z. Zheng, O.-S. Lee, W. Shim, G. Zheng, G. C. Schatz and C. A. Mirkin, *Nano Lett.*, 2010, **10**, 4399.
2 D. Credgington, O. Fenwick, A. Charas, J. Morgado, K. Suhling and F. Cacialli, *Adv. Funct. Mater.*, 2010, **20**, 2842.
3 F. Huo, G. Zheng, X. Liao, L. R. Giam, J. Chai, X. Chen, W. Shim and C. A. Mirkin, *Nat. Nanotechnol.*, 2010, **5**, 637.
4 M. Kiffner, J. Evers and M. S. Zubairy, *Phys. Rev. Lett.*, 2008, **100**, 073602.
5 J. K. W. Yang, Y. S. Jung, J.-B. Chang, R. A. Mickiewicz, A. Alexander-Katz, C. A. Ross and K. K. Berggren, *Nat. Nanotechnol.*, 2010, **5**, 256.
6 A. A. Shestopalov, R. L. Clark and E. J. Toone, *Nano Lett.*, 2010, **10**, 43.
7 R. C. Shallcross, G. S. Chawla, F. S. Marikkar, S. Tolbert, J. Pyun and N. R. Armstrong, *ACS Nano*, 2009, **3**, 3629.
8 A. Perl, D. N. Reinhoudt and J. Huskens, *Adv. Mater.*, 2009, **21**, 2257.
9 S. S. Williams, S. Retterer, R. Lopez, R. Ruiz, E. T. Samulski and J. M. DeSimone, *Nano Lett.*, 2010, **10**, 1421.
10 E. A. Costner, M. W. Lin, W.-L. Jen and C. G. Willson, *Annu. Rev. Mater. Res.*, 2009, **39**, 155.
11 L. Li, T. Y. Zhai, H. B. Zeng, X. S. Fang, Y. Bando and D. Golberg, *J. Mater. Chem.*, 2011, **21**, 40.
12 L. C. Jia and W. P. Cai, *Adv. Funct. Mater.*, 2010, **20**, 3765.
13 G. Zhang and D. Wang, *Chem.–Asian J.*, 2009, **4**, 236.
14 J. H. Zhang, Y. F. Li, X. M. Zhang and B. Yang, *Adv. Mater.*, 2010, **22**, 4249; Y. Lei, W. P. Cai and G. T. Duan, *Chem. Mater.*, 2008, **20**, 615.
15 Y. Lei, S. Yang, M. Wu and G. Wilde, *Chem. Soc. Rev.*, 2011, **40**, 1247.
16 N. D. Denkov, O. D. Velev, P. A. Kralchevsky, I. B. Ivanov, H. Yoshimura and K. Nagayama, *Langmuir*, 1992, **8**, 3183.
17 A. S. Dimitrov and K. Nagayama, *Langmuir*, 1996, **12**, 1303.
18 U. Ch. Fischer and H. P. Zingsheim, *J. Vac. Sci. Technol.*, 1981, **19**, 881.
19 H. W. Deckmann and J. H. Dunsmuir, *Appl. Phys. Lett.*, 1982, **41**, 377.
20 H. W. Deckmann and J. H. Dunsmuir, *J. Vac. Sci. Technol., B*, 1983, **1**, 1109.
21 C. L. Haynes and R. P. van Duyne, *J. Phys. Chem. B*, 2001, **105**, 5599.
22 T. R. Jensen, M. D. Malinsky, C. L. Haynes and R. P. van Duyne, *J. Phys. Chem. B*, 2000, **104**, 10549.
23 C. L. Haynes, A. D. McFarland, M. T. Smith, J. C. Hulteen and R. P. van Duyne, *J. Phys. Chem. B*, 2002, **106**, 1898.
24 X. Zhang, E. M. Hicks, J. Zhao, G. C. Schatz and R. P. van Duyne, *Nano Lett.*, 2005, **5**, 1503.
25 G. H. Chan, J. Zhao, E. M. Hicks, G. C. Schatz and R. P. Van Duyne, *Nano Lett.*, 2007, **7**, 1947.
26 W. Huang, W. Qian and M. A. El-Sayed, *Nano Lett.*, 2004, **4**, 1741.
27 G. Zhang and D. Wang, *J. Am. Chem. Soc.*, 2008, **130**, 5616.
28 K. Kempa, B. Kimball, J. Rybczynski, Z. P. Huang, P. F. Wu, D. Steeves, M. Sennett, M. Giersig, D. V. G. L. N. Rao, D. L. Carnahan, D. Z. Wang, J. Y. Lao, W. Z. Li and Z. F. Ren, *Nano Lett.*, 2003, **3**, 13.
29 B. Fuhrmann, H. S. Leipner and H. Höche, *Nano Lett.*, 2005, **5**, 2524.
30 C. M. Zhou and D. Gall, *Thin Solid Films*, 2007, **516**, 433.
31 H. Zeng, X. Xu, Y. Bando, U. K. Gautam, T. Zhai, X. Fang, B. Liu and D. Golberg, *Adv. Funct. Mater.*, 2009, **19**, 3165.
32 C. Li, G. Hong, P. Wang, D. Yu and L. Qi, *Chem. Mater.*, 2009, **21**, 891.
33 A. Kosiorek, W. Kandulski, H. Glaczynska and M. Giersig, *Small*, 2005, **1**, 439.
34 A. Kosiorek, W. Kandulski, P. Chudzinski, K. Kempa and M. Giersig, *Nano Lett.*, 2004, **4**, 1359.
35 M. C. Gwinner, E. Koroknay, L. Fu, P. Patoka, W. Kandulski, M. Giersig and H. Giessen, *Small*, 2009, **5**, 400.
36 M. Bowker, M. Broughton, A. Carley, P. Davies, D. Morgan and J. Crouch, *Langmuir*, 2010, **26**, 16261.
37 U. Thiele, M. Mertig and W. Pompe, *Phys. Rev. Lett.*, 1998, **80**, 2869.
38 C. Favazza, J. Trice, H. Krishna and R. Kalyanaraman, *Appl. Phys. Lett.*, 2006, **88**, 153118.
39 S. Yang, F. Xu, S. Ostendorp, G. Weilde, H. Zhao and Y. Lei, *Adv. Funct. Mater.*, 2011, DOI: 10.1002/adfm.201002387.
40 G. Duan, W. Cai, Y. Luo, Y. Li and Y. Lei, *Appl. Phys. Lett.*, 2006, **89**, 181918.
41 N. Wang, Y. Cai and R. Q. Zhang, *Mater. Sci. Eng., R*, 2008, **60**, 1.
42 G. Z. Shen and D. Chen, *Nanoscale Res. Lett.*, 2009, **4**, 779.
43 Y. Xia, P. Yang, Y. Sun, Y. Wu, B. Mayers, B. Gates, Y. Yin, F. Kim and Y. Yan, *Adv. Mater.*, 2003, **15**, 353.
44 X. H. Hu and C. T. Chan, *Appl. Phys. Lett.*, 2004, **85**, 1520.
45 T. S. Kang, A. P. Smith, B. E. Taylor and M. F. Durstock, *Nano Lett.*, 2009, **9**, 601.
46 S. V. Kesapragada and D. Gall, *Thin Solid Films*, 2006, **494**, 234.
47 C. M. Zhou and D. Gall, *Thin Solid Films*, 2006, **515**, 1223.
48 Y. Li, T. Sadaki, Y. Shimizu and N. Koshizaki, *J. Am. Chem. Soc.*, 2008, **130**, 14755.
49 Y. Li, X. Fang, N. Koshizaki, T. Sadaki, L. Li, S. Gao, Y. Shimizu, Y. Bando and D. Golberg, *Adv. Funct. Mater.*, 2009, **19**, 2467.
50 Y. Li, T. Sadaki, Y. Shimizu and N. Koshizaki, *Small*, 2008, **4**, 2286.
51 L. Li and N. Koshizaki, *J. Mater. Chem.*, 2010, **20**, 2972.
52 L. Li, Y. Li, S. Y. Gao and N. Koshizaki, *J. Mater. Chem.*, 2009, **19**, 8366.
53 Y. Li, J. Zhang, S. Zhu, H. Dong, F. Jia, Z. Wang, Z. Sun, L. Zhang, Y. Li, H. Li, W. Xu and B. Yang, *Adv. Mater.*, 2009, **21**, 4731.
54 X. Zhang, J. Zhang, Z. Ren, X. Li, X. Zhang, D. Zhu, T. Wang, T. Tian and B. Yang, *Langmuir*, 2009, **25**, 7375.
55 X. Wang, C. J. Summers and Z. L. Wang, *Nano Lett.*, 2004, **4**, 423; D. F. Liu, Y. J. Xiang, Q. Liao, J. P. Zhang, X. C. Wu, Z. X. Zhang, L. F. Liu, W. J. Ma, J. Shen, W. Y. Zhou and S. S. Xie, *Nanotechnology*, 2007, **18**, 405303.
56 R. M. Anisru, J. Shin, H. H. Choi, K. M. Yeo, E. J. Kang and I. S. Lee, *J. Mater. Chem.*, 2010, **20**, 10615.
57 Z. L. Schaefer, M. L. Gross, M. A. Hickner and R. E. Schaak, *Angew. Chem., Int. Ed.*, 2010, **49**, 7045.
58 X. Wang, X.-L. Wu, Y.-G. Guo, Y. Zhong, X. Cao, Y. Ma and J. Yao, *Adv. Funct. Mater.*, 2010, **20**, 1680.
59 S. Yang, X. Feng, L. Zhi, Q. Cao, J. Maier and K. Müller, *Adv. Mater.*, 2010, **22**, 838.

60 K. Y. Niu, J. Yang, S. A. Kulinich, J. Sun, X. Wu and Du, *Langmuir*, 2010, **26**, 16652.
61 G. Duan, F. Lv, W. Cai, Y. Luo, Y. Li and G. Liu, *Langmuir*, 2010, **26**, 6295.
62 J. Elias, C. Levy-Clement, M. Bechelany, J. Michler, G.-Y. Wang, Z. Wang and L. Philippe, *Adv. Mater.*, 2010, **22**, 1607.
63 G. Duan, W. Cai, Y. Li, Z. Li, B. Cao and Y. Luo, *J. Phys. Chem. B*, 2006, **110**, 7184.
64 S. Yang, W. Cai, J. Yang and H. Zeng, *Langmuir*, 2009, **25**, 8287.
65 S. Yang, W. Cai, L. Kong and Y. Lei, *Adv. Funct. Mater.*, 2010, **20**, 2527.
66 X. Wang, C. Lao, E. Graugnard, C. J. Summers and Z. L. Wang, *Nano Lett.*, 2005, **5**, 1784.
67 C. Wang, W. Ruan, N. Ji, W. Ji, S. Lv, C. Zhao and B. Zhao, *J. Phys. Chem. C*, 2010, **114**, 2886.
68 Y. Li, J. Zhang, T. Wang, S. Zhu, H. Yu, L. Fang, Z. Wang, L. Cui and B. Yang, *J. Phys. Chem. C*, 2010, **114**, 19908.
69 M. Xu, N. Lu, H. Xu, D. Qi, Y. Wang and L. Chi, *Langmuir*, 2009, **25**, 11216.
70 S. Yang, Y. Lei, submitted results.
71 Y. Li, C. Li, S. O. Cho, G. Duan and W. Cai, *Langmuir*, 2007, **23**, 9802.
72 F. Sun and J. C. Yu, *Angew. Chem., Int. Ed.*, 2007, **46**, 773.
73 J. S. Levy, A. Gondarenko, M. A. Foster, A. C. Turner-Foster, A. L. Gaeta and M. Lipson, *Nat. Photonics*, 2009, **4**, 37.
74 X. Wu, P. Jiang, Y. Ding, W. Cai, S.-S. Xie and Z. L. Wang, *Adv. Mater.*, 2007, **19**, 2319.
75 H. Jiang and J. Sabarinathan, *J. Phys. Chem. C*, 2010, **114**, 15243.
76 M. Bayati, P. Patoka, M. Giersig and E. R. Savinova, *Langmuir*, 2010, **26**, 3549.
77 Z. Sun, Y. Li, J. Zhang, Y. Li, Z. Zhao, K. Zhang, G. Zhang, J. Guo and B. Yang, *Adv. Funct. Mater.*, 2008, **18**, 4036.
78 E. Verhagen, R. Waele, L. Kuipers and A. Polman, *Phys. Rev. Lett.*, 2010, **105**, 223901.
79 W. Chen, A. Bian, A. Agarwal, L. Liu, H. Shen, L. Wang, C. Xu and N. A. Kotov, *Nano Lett.*, 2009, **9**, 2153.
80 Y. Lu, G. L. Liu, J. Kim, Y. X. Mejia and L. P. Lee, *Nano Lett.*, 2005, **5**, 119.
81 R. Bukasov, T. A. Ali, P. Nordlander and J. S. Shumaker-Parry, *ACS Nano*, 2010, **4**, 6639.
82 B. M. Ross and L. P. Lee, *Nanotechnology*, 2008, **19**, 275201.
83 M. Retsch, M. Tamm, N. Bocchio, N. Horn, R. Förch, U. Jonas and M. Kreiter, *Small*, 2009, **5**, 2105.
84 J. R. Oh, J. H. Moon, H. K. Park, J. H. Park, H. Chung, J. Jeong, W. Kim and Y. R. Do, *J. Mater. Chem.*, 2010, **20**, 5025.
85 C. Li, G. Hong and L. Qi, *Chem. Mater.*, 2010, **22**, 476.
86 S. Yang, Y. Lei, unpublished results.
87 A. Valsesia, T. Meziani, F. Bretagnol, P. Colpo, G. Ceccone and F. Rossi, *J. Phys. D: Appl. Phys.*, 2007, **40**, 2341.
88 A. Plettle, F. Enderle, M. Saitner, A. Manzke, C. Pfahler, S. Wiedemann and P. Ziemann, *Adv. Funct. Mater.*, 2009, **19**, 3279.
89 J. Yang, G. Duan and W. Cai, *J. Phys. Chem. C*, 2009, **113**, 3973.
90 M. Lopez-Garcia, J. F. Galisteo-Lopez, A. Blanco, C. Lopez and A. Garcia-Martin, *Adv. Funct. Mater.*, 2010, **20**, 4338.
91 Z. Huang, H. Fang and J. Zhu, *Adv. Mater.*, 2007, **19**, 744; X. Wang, K. L. Pey, W. K. Choi, C. K. F. Ho, E. Fitzgerald and D. Antoniadis, *Electrochem. Solid-State Lett.*, 2009, **12**, K73.
92 C. L. Cheung, R. J. Nikolic, C. E. Reinhardt and T. F. Wang, *Nanotechnology*, 2006, **17**, 1339.
93 T. M. Blattler, A. Binkert, M. Zimmermann, M. Textor, J. Voros and E. Reimhult, *Nanotechnology*, 2008, **19**, 075301.
94 M. A. Ray and L. Jia, *Adv. Mater.*, 2007, **19**, 2020; K. D. Danov, P. A. Kralchevsky and M. P. Boneva, *Langmuir*, 2006, **22**, 2653; M. A. Ray, N. Shewmon, S. Bhawalkar, L. Jia, Y. Yang and E. S. Daniels, *Langmuir*, 2009, **25**, 7265; L. Isa, K. Kumar, M. Muller, J. Grolig, M. Textor and E. Reimhult, *ACS Nano*, 2010, **4**, 5665; S. P. Bhawalkar, J. Qian, M. C. Heiber and L. Jia, *Langmuir*, 2010, **26**, 16662; N. Aubry, P. Singh, M. Janjua and S. Nudurupati, *Proc. Natl. Acad. Sci. U. S. A.*, 2008, **105**, 3711.
95 A. Unger, U. Rietzler, R. Berger and M. Kreiter, *Nano Lett.*, 2009, **9**, 2311.
96 N. Vogel, M. Jung, N. L. Bocchio, M. Retsch, M. Kreiter and I. Köper, *Small*, 2010, **6**, 104.
97 G. Hong, C. Li and L. Qi, *Adv. Funct. Mater.*, 2010, **20**, 3774.
98 L. Jia, W. Cai, H. Wang, F. Sun and Y. Li, *ACS Nano*, 2009, **3**, 2697.
99 L. Jia, W. Cai and H. Wang, *J. Mater. Chem.*, 2009, **19**, 7301.
100 L. Jia, W. Cai and H. Wang, *Appl. Phys. Lett.*, 2010, **96**, 103115.
101 X. H. Xia, J. P. Tu, J. Zhang, J. Y. Xiang, X. L. Wang and X. B. Zhao, *ACS Appl. Mater. Interfaces*, 2010, **2**, 186.
102 Y. F. Yuan, X. H. Xia, J. B. Wu, J. L. Yang, Y. B. Chen and S. Y. Guo, *Electrochem. Commun.*, 2010, **12**, 890.
103 J. Y. Xiang, X. L. Wang, X. H. Xia, J. Zhong and J. P. Tu, *J. Alloys Compd.*, 2011, **509**, 157.
104 X. Li, J. Li, T. Chen, B. K. Tay, J. Wang and H. Yu, *Nanoscale Res. Lett.*, 2010, **5**, 1721.
105 M. Chigane, M. Watanabe, M. Izaki, I. Yamaguchi and T. Shinagawa, *Electrochem. Solid-State Lett.*, 2009, **12**, E5.
106 B. Bhushan and Y. C. Jung, *Prog. Mater. Sci.*, 2011, **56**, 1.
107 K. Liu, X. Yao and L. Jiang, *Chem. Soc. Rev.*, 2010, **39**, 3240.
108 Y. Li, J. Zhang, S. Zhu, H. Dong, Z. Wang, Z. Sun, J. Guo and B. Yang, *J. Mater. Chem.*, 2009, **19**, 1806.
109 N. Shang, P. Papakonstantinou, P. Wang, A. Zakharov, U. Palnitkar, I.-N. Lin, M. Chu and A. Stamboulis, *ACS Nano*, 2009, **3**, 1032.
110 C.-M. Chang, Y.-C. Chang, C.-Y. Lee, P.-H. Yeh, W.-F. Lee and L.-J. Chen, *J. Phys. Chem. C*, 2009, **113**, 9153.
111 T. Mueller, F. N. A. Xia and P. Avouris, *Nat. Photonics*, 2010, **4**, 297.
112 G. Diamant, E. Halahmi, L. Kronik, J. Levy, R. Naaman and J. Roulston, *Appl. Phys. Lett.*, 2008, **92**, 262903.
113 W. li, J. Zhou, X. Zhang, J. Xu, L. Xu, W. Zhao, P. Sun, F. Song, J. Wan and K. Chen, *Nanotechnology*, 2008, **19**, 135308.
114 Y. Li, J. Zhang and B. Yang, *Nano Today*, 2010, **5**, 117.
115 Z. P. Huang, H. Fang and J. Zhu, *Adv. Mater.*, 2007, **19**, 744.
116 Y. Li, J. Zhang, S. Zhu, H. Dong, Z. Wang, Z. Sun, J. Guo and B. Yang, *J. Mater. Chem.*, 2009, **19**, 1806.
117 X. Wang, X. Yan and C. Kan, *J. Mater. Chem.*, 2011, **21**, 4251.

